 doi:10.20944/preprints202107.0431.v1

Article

Natural-Fibrous lime-based mortar for the rapid retrofitting of masonry heritage

Marco Vailati [1,*], Micaela Mercuri [1] Michele Angiolilli [2] Amedeo Gregori [1]

[1] Department of Civil, Construction and Environmental Engineering, University of L'Aquila, 67100 L'Aquila; marco.vailati@univaq.it, amedeo.gregori@univaq.it, micaela.mercuri@graduate.univaq.it.
[2] Department of Civil, Environmental and Chemical Engineering, University of Genoa, 16145 Genoa; michele.angiolilli@edu.unige.it
* Correspondence: marco.vailati@univaq.it

Abstract: The present work aims to characterize the mechanical behavior of a new composite material for the conservation and development of the vast historical and architectural heritage that is particularly vulnerable to environmental and seismic actions. The new composite consists of natural hydraulic lime (NHL) -based mortar, reinforced by sisal short fibers randomly oriented in the mortar matrix. The NHL-based mortar ensures the chemical-physical compatibility with the original feature of the historical masonry structures (mostly in stone and clay) aiming to pursue both the effectiveness and durability of the intervention. The use of vegetable fibers (i.e. the sisal one) is an exciting challenge for the construction industry since they require a lower degree of industrialization for their processing, and therefore, their costs are also low, as compared to the most common synthetic/metal fibers. Beams of sisal-composite sizing 160x40x40 mm^3 with a central notch are tested in three-point bending, aiming to evaluate both their bending strength and fracture energy. Also, tensile tests and compressive tests were performed on the composite samples, while water retention test and slump test were performed on the fresh mix. Finally, the tensile tests on the Sisal strand were carried out to evaluate the tensile strength of both strand and wire. A final comparison with unreinforced mortar specimens shows that the proposed composite ensures great workability and good performances in term of ductility and strength and it can be considered a promising alternative to the classic fiber-reinforcing systems.

Keywords: masonry; composite; short fibers; natural hydraulic lime; sisal; three-point bending test; fracture energy; strengthening; preservation; sustainability; carbon foot print

1. Introduction

Masonry structures constitute a significant part of the most valuable existing historical and artistic real estate heritage around the world. These structures are particularly vulnerable to environmental and seismic actions, as highlighted during recent calamities (e.g. Kashmir 2005, L'Aquila 2009, Christchurch 2011, Emilia 2012, Amatrice 2016). Under earthquake excitation, masonry structures are subjected to multi-directional ground motions, which causes in-plane and out-of-plane loads and eventually provokes their collapse [1-8]. In the last decade, there has been a growing demand in protecting masonry heritages because of decades of studies and investments in this field as well as the necessity to maintain and to pass them to future generations.

Nowadays, fiber-based strengthening systems are commonly adopted for the repair and reinforcement of historic masonry structures as an alternative to traditional systems (i.e. reinforced drilling or steel-reinforced concrete plaster). Despite the development of the fiber-based strengthening system began in the 1960s [9], this technology has been commonly adopted for masonry only in the last decade because of the increasingly strict rules required by conservation committees for heritage preservation. Indeed, the efficiency of the strengthening system is now required in combination with low invasiveness of the strengthening solution and high compatibility with the original structures.

Among modern and innovative solutions of intervention on existing structures, composite materials, such as the Fiber Reinforced Polymers (FRP) [10] or the Fiber Reinforced Cementitious Matrix (FRCM) [11,12], have been increasingly considered for the strengthening of both modern and historic masonry constructions (buildings, bridges, towers) and individual structural components (walls, arches and vaults, pillars, and columns). These technologies comprise the use of composites material characterized by uni or bi-directional long fibers. These materials are proven to be effective in increasing the load-carrying capacity of masonry elements and improving their structural behavior through a reduction of critical brittle failure modes. Most importantly, the increase in strength is obtained with a lower increment of the structural weight, as compared to the traditional ones (e.g., steel-reinforced concrete plaster). For the global strengthening of historical masonry, the use of the FRCM is more adequate than the use of FRP because of the irregular surface of the masonry substratum and the typical disaggregation failure of that structure [13-17] as well as the issues of the FRP related to the use of epoxy adhesives (incompatibility with the original constituent material of the masonry structure, reversibility of the intervention, durability) [18,19].

A common disadvantage of both the FRCMs and FRPs concerns the orientation of the fibers in specific directions: the FRCMs are characterized by fiber strands oriented in a bidirectional way; the FRPs are characterized by a prior defined fiber direction (usually along the diagonal and the edges of the walls). It is worth noting that fibers activate their excellent tensile properties along their axial direction, whereas they have negligible properties in the other directions (e.g. [20]). However, tensional states induced by seismic events do not act in a single and defined direction, and therefore the classic fiber-based systems may not be very efficient.

The present work is part of a larger research program that investigates the repair/strengthening systems for the historical and architectural masonry heritage through sustainable composite materials by replacing: (i) the cementitious nature of the classic strengthening system with the lime-based material; (ii) the most used inorganic or synthetic fibers with organic natural ones. In particular, the new composite was developed by using a natural hydraulic lime (NHL) mortar, reinforced by short sisal fibers randomly oriented in the mortar matrix.

Using NHL-based mortar aims to ensure the chemical-physical compatibility with the original feature of the historical masonry structures (mostly in stone and clay) to pursue both the effectiveness and durability of the intervention [21-23]. Indeed, the NHL-based mortar is considered a promising alternative to cement materials when high compatibility with historical substrates is strictly required. The proposed composite is conceived to be applied as a coating on masonry surfaces, presenting greater advantages in terms of easiness and time application in situ, as compared to the other classical fiber-systems. Suffice it to say that it can be applied in a unique phase, consisting of the application of a single layer of the product to the masonry surface. This would consistently reduce the cost and the impact of seismic and energy retrofit of built heritage.

Incorporation of fibers into mortar/concrete materials can significantly improve the tensile strength, ductility, toughness, and durability of the material by preventing or controlling the initiation and propagation of cracks [24] thanks to the fiber bridging mechanism.

Furthermore, the introduction of short fibers reduces the use of the cement/lime materials with a consequent reduction in production (and soil consumption) and energy consumption. Indeed, the cement and lime production processes are energy-intensive and produce plenty of CO_2.

The mechanical behavior of lime-based mortar (reproducing the compositions of historical one) and reinforced by randomly oriented short glass fibers was investigated in [23]. The results obtained with various types/content of fibers in binders highlighted that composites ensure increased strength and excellent ductility capacity, thus making them

 doi:10.20944/preprints202107.0431.v1

a promising alternative to traditional (long) fiber reinforcement systems, even for ancient constructions.

The use of the fibers of different nature (steel, carbon, aramid, plastic, glass, cast iron, polypropylene, polyacrylonitrile, polyolefin, etc.) is usually adopted for high-performance applications, such as automobiles and aircraft industries, and is greatly increased for concrete structures (e.g., industrial concrete slabs, structural or nonstructural precast elements, and tunnel coatings).

However, the high-performance of composites with metallic/synthetic fibers are difficult to recycle as the separation of the components is quite difficult to perform. This has often led to unsatisfactory disposal of those materials that cause vast environmental impact [25-27]. Furthermore, it is worth noting that these materials are non-renewable resources.

Academic and industrial efforts are continuously engaged to develop new materials that can provide efficient alternatives to conventional construction materials and improve the energy efficiency in buildings or can repair and protect existing structures. This new generation of materials, before an actual market entry, needs to be carefully analyzed, especially in their long-term performance.

Using vegetable fibers in the mortar (or concrete) is an exciting challenge for the construction industry since they require only a low degree of industrialization for their processing and therefore, they are cheap compared to the conventional metallic/synthetic fibers. Furthermore, the advantage of using natural fiber is that it is readily available and environmentally friendly.

Natural fiber-reinforced composites are emerging very rapidly thanks to developments in research aimed to improve the durability limitations, as treatments and coating systems [27,28]. Natural fibers can replace conventional metallic/synthetic fibers in several applications [28-40] although they are mainly adopted for non-structural components such as roofing tiles, concrete masonry blocks, slab for roofing, and construction of water tanks [39].

The most used natural fibers in the civil engineering field are sisal, henequen, coconut, flax, bamboo, hemp, jute, ramie, wood, palm, banana, and pineapple. In particular, natural fibers composites show good mechanical properties, implying reduced thickness and low weight.

The low elasticity modulus of natural fiber improves the energy absorption of composites in the post-cracking behavior. Indeed, randomly distributed short fibers in quasi-brittle matrices (i.e. mortar or concrete) can significantly improve the response to impact solicitation due to the enormous ability for dynamic energy dissipation [40-42]. The main differences observed for the various natural fibers is well described in [43] in terms of: (i) hygric, chemical and mechanical structure; (ii) fiber-cement composite properties and performance; (iii) enhancement of the properties of plant-based fiber reinforced cement composites.

In the present work, the sisal fibers were adopted, aiming to improve the mechanical properties of the lime-based reinforcing mortar.

Sisal fiber is a hard fiber extracted from the leaves of the sisal plant (*Agave sisalana*). Though native to tropical and subtropical North and South America, the sisal plant is now widely grown in tropical countries of Africa, the West Indies, and the Far East. Nearly 4.5 million tons of sisal fiber are produced every year throughout the world, especially in Tanzania and Brazil [37,38]. In general, a sisal plant produces about 200 - 250 leaves and each leaf (weighing about 600 g) contains about 1000 fiber bundles (about 3% by weight; it is worth noting that 90% is water) [44]. It is worth noting that the cost of sisal fibers per unit weight is about 10% of the cost of glass fiber, although the mechanical properties of sisal fiber are clearly lower than glass fiber [45].

Regarding the mechanical characterization of sisal fibers, a study [37] concluded that no significant variation of mechanical properties was observed in the tensile test by varying the fiber diameter. However, both the tensile strength and the ultimate elongation

decrease while Young's modulus increases with fiber length. In that research, it was also highlighted the dependency of the mechanical behavior of the sisal to the test speed. Indeed, for high strain rates (500 mm/min) one can observe a sudden fall in tensile strength mainly because of the presence of imperfections in the fiber causing immediate failure. On the contrary, at very slow test speeds, the fiber behaves like a viscous liquid because of the internal microstructure of the fiber. The effect of the test speed on the mechanical properties of the fibers was also found in [38] for other natural fibers (i.e. the sun-hemp one).

The mechanical properties of sisal fibers obtained from different age at three different temperature were investigated in [46]. Results showed a decrease of the tensile strength, modulus and toughness values of the sisal fiber for increasing temperature and mainly attributed to the more intense removal of water and/or other volatiles originally present in the fibers, which otherwise act as plasticizing agents in the chains of the cellulose macromolecule.

Tensile strength of sisal fibers decreases up to 50% if immersed in a PH12 solution for 28 days [40]. Hence, to avoid aging effects in the composites, some approaches should be adopted, such as an application of a protective coating, high casting compaction for providing matrix carbonation (with the addition of silica fume if necessary), and use of clow alkaline binders based on blast furnace slag and fly ash (e.g. [47]). In [40] is well described the effect of various treatments on the composite properties.

Furthermore, several researchers investigated the properties of composites reinforced by sisal fibers. In [48] a cementitious matrix reinforced with untreated bi-directional fabrics of sisal fibers were mechanically characterized by tensile tests performed on both single yarns and composite strips. Results showed good adhesion of those fibers with the mortar matrix, demonstrating an appreciable ductile behavior and moderate tensile strength for such composites.

Cement-based composites reinforced with long unidirectional aligned sisal fibers under both direct tensile and bending tests aiming to determine the first crack, post-peak strength, and toughness of the composites were investigated in [49]. Results showed the potential of the use of that fiber type for semi-structural and structural applications. Furthermore, it was highlighted that drying shrinkage in the mortar can increase with the presence of sisal fibers, as the porous nature of the fiber, at the microstructure level, created more moisture paths into the matrices leading to higher drying shrinkage.

The mechanical behavior of cement mortar reinforced by sisal fiber with different lengths was investigated in [50]. The results indicated that the introduction of the fibers leads to a decrease in compressive strength and an increase of the fracture toughness (the latter proportional to the fiber length), as compared to the plain cement mortar.

From another research [51], it was also highlighted that the addition of short sisal fibers to cement matrices tends to reduce the peak stress, strain at failure, and elastic modulus of the matrix and increase the toughness of the matrix. Furthermore, the elastic properties (peak stress, elastic modulus, and peak strain) of the composites reinforced with sisal fiber 50 mm long were smaller than those obtained with fiber 25 mm long. The toughness index, on the other hand, was less affected by the increase in the fiber length.

A reinforcement consisted of sisal fibers yarns impregnated with a water-based resin and embedded in an inorganic matrix based on natural lime was tested under both tensile and single-lap shear tests [52]. For the impregnated yarns, the mechanical characterization of the composite evidenced an elastic-brittle behavior with a higher tensile strength with respect to dry fibers yarns (difference of about 15%), due to a more uniform distribution of the stresses among the fibers. In single-lap shear tests, a progressive, the tensile failure of the yarns was always attained, and no slip was observed at the masonry-mortar interface. This behavior was due to the adequate bond length (260 mm) that avoided debonding or sliding failures.

Cement- based composite (with partial replacement of Portland cement by 30% of metakaolin and 20% of calcined waste crushed clay brick to improve the durability)

Preprints (www.preprints.org) | NOT PEER-REVIEWED | Posted: 20 July 2021 doi:10.20944/preprints202107.0431.v1

reinforced by long sisal fibers was investigated in [53]. The mechanical response of the composed was measured under both tension and bending tests. The composites showed high modulus (more than 30 GPa) at linear-elastic zones ranges and ultimate strengths of 12 and 25 MPa under tension and bending tests, respectively.

A comparison between sisal, jowar and bamboo fibers embedded in a polyester resin matrix and tested under both tensile and bending tests was proposed in [54]. In that research, the better performance of the jowar fibers was observed, suggesting the idea to propose that comparison in future research also for mortar-based composite instead of the polyester resin one.

The mechanical characterization of the proposed composite, defined by a lime-based mortar strengthened by short sisal fibers randomly diffused in the mortar matrix, was experimentally performed and discussed in this paper. Beams with dimensions of 160x40x40 mm^3 with a central notch were tested in three-point bending, aiming to evaluate both the bending strength and the fracture energy of the composite material. Then, compression tests were conducted using 80x40x40 mm^3 prismatic mortar specimens obtained from the two-half specimens tested in three-point bending.

2. Test campaign

In this study, Sisal fibers derived from Aloe plants were employed. In particular, the ratio between the length and the average diameter of the fibers and the fiber content on both the tensile and compressive strengths, as well as the workability of the mixture were investigated. Authors paid special attention to the fibers selecting, chosen on the base of their length l_f. In fact, is known from the literature that the higher fiber length, the higher the mechanical properties of the mixture and the lower the workability; in particular, the negative effects of the long fibers occur in the mixing phase and especially when the mixture is applied with spraying technique on the masonry surface (almost the unique possible application of this kind of product).

Following their recent work on the reinforced lime-base mortar with glass fibers [23], authors have defined two sets test with two different fibers length, 24 mm and 13 mm, respectively named F1 and F2. At the time, the low spread of this kind of fibers does not allow an industrial develop than it can provide the fibers according to the needs of the user. Therefore almost all companies who work in this field provide the Sisal wires under shape of spiral strand in woven fabric or wrapped in reels, as shown in figure 1.

The spiral strand with 2 mm diameter is carefully cut to the predefined length (24 mm and 13 mm) and unwrapped until to obtain single fibers with an effective diameter equal to 0.028 mm, measured via stereo microscope as shown in the picture of figure 2.

As opposed to found in [23] about the glass fibers, here the Sisal fibers wouldn't seem treated with any impregnation, at least to visual and tactile inspection.

Geometrical and mechanical parameters are summarizing in the following table 1, where l_f is the fiber length, d_f is the diameter of the single yarn, d_f^* is the diameters of the strand, ρ_{fib} is the density, E_f is the Young's module, $f_{t,f}$ is the ultimate tensile strength and $\varepsilon_{u,f}$ is the ultimate strain. The first two parameters and $f_{t,f}$ have been directly evaluated on the fibers and from technical datasheet, while the density is taken from literature. It is worth to noting that the ultimate tensile strength $f_{t,f}$ evaluate by testing, matches the values from literature.

Table 1. Geometrical and mechanical properties of the Sisal fibers used in the experiments.

Name	l_f [mm]	d_f [mm]	d^*_f [mm]	ρ_{fib} [kN/m^3]	$f_{t,f}$ [MPa]
F1	24	0.28	2.0	10.6	130
F2	13				

 doi:10.20944/preprints202107.0431.v1

Four components have been used to realize the dry mortar: binders, chemicals, fibers and aggregates, exactly mixed following the same order; water was added as last component during the mixing phase. The sieve curve for aggregates includes sand with size ranging from 0.1 mm to 1.2 mm. The mixture ratio design is given in Table 2.

Table 2. Mixture ratio of the mortar.

Family	*Component*	*%*
Binders[1]	Lime	30
	Portland cement	70
Chemicals[2]	Fluidizer	0.2
	Resin	0.1
Fibers[2]	Sisal	0.6, 0.75, 1.00
Aggregates[2]	Sand	65
-	Water	20[2] (80)[2]

[1] Respect the total weight of the binder
[2] Respect the total weight of the product

Having been mixed by the mortar mixer, the mortar was cast in the three-gang prism mould measuring 160 mm in length, 40 mm in height and 40 mm in thickness each and vibrated according to the standard code EN 1015-11 [55]. As final step, the three samples are subjected to the slump test (section 3.1) to evaluate the workability. For the next 48 hours the samples were kept moist on the shelves in a conservation room where the temperature is kept under steady condition (20±2°) and the relative humidity is kept above 95% by atomization. At the end of this first step, the molds were removed and the specimens were left in laboratory condition for 26 days with room temperature and relative humidity of 20° and 60 %, respectively. After 28 days the specimens are subjected to three-point bending test (section 3.2) and each couple of pieces of the broken sample were used to determine tensile strength section 3.3) and compressive strength section 3.4). Testing procedure is explained in the next paragraph.

Test campaign has engaged a total of 53 mortar samples, three unreinforced and 50 fibrous mortar samples (nine samples for each three-fiber content for both length, except for the set with fiber content 0.75% and fiber type F1 where 5 specimens have been done).

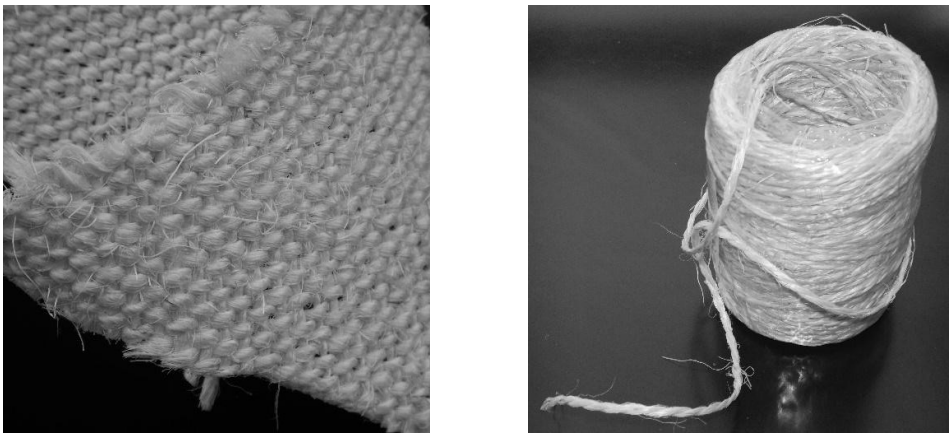

(**a**) (**b**)

Figure 1. The two most common shapes of fibers commercially available: (**a**) woven fabric; (**b**) reels. They are briefly named as RM1 and RM2, respectively, in the water retention test.

 doi:10.20944/preprints202107.0431.v1

Figure 2. 40X magnification of Sisal wire with Leica stereo microscope. Scale in micrometer (1 m= 0.001 mm)

Starting from the shapes shown in figure 1, fibers were unwrapped and cutted. Figure 3 shows the work steps through which fibers were obtained.

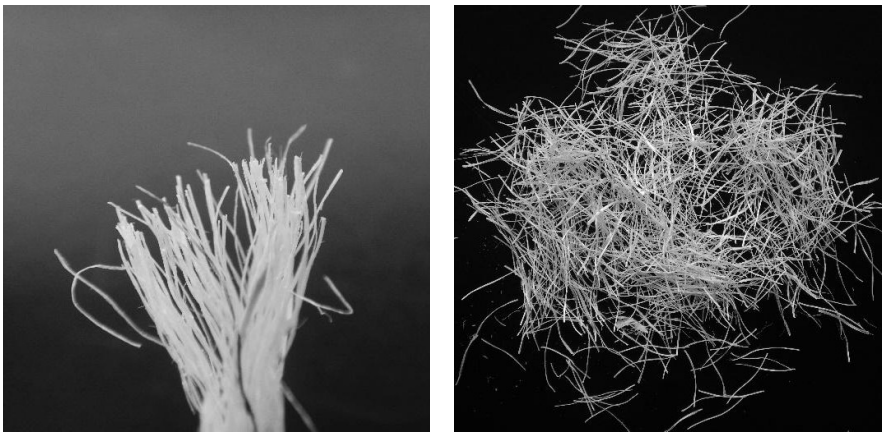

a) (**b**)

Figure 3. Fibers preparation steps: (**a**) unwrapped of spiral strand; (**b**) 13 mm short fibers after cutting.

In order to better investigate the effect of the fibers on the mechanical properties of the mortar, as done in their previous work [23], authors decided to keep the limit of lime at 30% with the goal to reduce the dispersion of the data. Indeed, it's noted from literature that the natural hydraulic lime (NHL) is affected by the higher variability of its mechanical properties respect the cement. Consequently, the mixture obtained it's more properly defined as "lime-based", rather than "pure-lime mortar".

The effect on the mechanical properties of the mixture was studied using different fibers density, in particular three percentages of fibers were taken: 0.6%, 0.75% and 1.00% of the total weight of the product. Table 3 summarizes the aspect ratio of the fibers compared with the total weight and volume of the single specimen.

Preprints (www.preprints.org) | NOT PEER-REVIEWED | Posted: 20 July 2021 doi:10.20944/preprints202107.0431.v1

Table 3. Fibers aspect ratio compared with a mortar specimen of dimensions 40x40x160 mm.

Name	l_f [mm]	*% respect the total weight*	*Fibers number*	*Fibers volume* [mm³]	*% respect the total volume*
F1	24	0.60	1965	2830	1.0
		0.75	2457	3538	1.3
		1.00	3276	4717	1.7
F2	13	0.60	3627	2829	1.0
		0.75	4534	3537	1.3
		1.00	6045	4715	1.7

Fiber weight and volume of 13 mm length: $8.27 \oplus 10^{-4}$ g/0.78 mm³
Fiber weight and volume of 24 mm length: $15.26 \oplus 10^{-4}$ g//1.44 mm³

It is worth notice that unreinforced specimens with the same mix design of the reinforced ones have been made. Therefore, any increase of mechanical properties of the fibrous mortar is due only by the fiber content.

3 Performances appraisal methods

Tests are conducted on the fresh and hardened mortar in reinforced and unreinforced configuration, and on the Sisal fibers in the form of strands. Just the last paragraph refers to the Sisal fibers, while the other paragraphs refer to the mortar in the mentioned configurations.

3.1 Evaluation of the workability

Fresh concrete or mortar properties are generally tested via slump test, the most widely used test for assessing the workability of concrete of normal consistency (where slump is ranging from 10 mm to 200 mm).

When the expected values are closely to the upper bound, the flow table test represent the better method to check the consistency of the mortar.

More specifically, both method aims to assess the consistency of freshly made mortar immediately before to cast of the batch in the mould, measuring its tendency to flow.

From practical point of view, the test has been performed following the procedure reported in the code EN 1015-3 [56] and ASTM C1437 [57] and using the Hagermann's flow table to shake each batch of mortar.

3.2 Water retention test

The fiber acts as a structural reinforcement for quasi-brittle materials, serving as a bridge for stress transfer in the cracks that may appear in the mortar matrix. However, the use of fibers reduces the fluidity of the material, which can cause negative impact in the workability of the mixture in the fresh state. Among other reasons, the workability reduction is due to the fact that the fibers partially absorb the water present in the mortar mixture. Thus, understanding the amount of water retained by the fibers when they are dispersed in the mortar matrix is fundamental. With this aim, the water retention test, regulated by the UNI-EN 459-2 [58], is a powerful methodology that can be adopted.

Specifically, in this section two water retention tests are performed on: (i) an unreinforced lime-based mortar and (ii) the same lime-based mortar reinforced with natural dispersed fibers. Expressing the water retention (wr) as the percentage of water which remains in the mortar mixture after short suction time, the difference between the water retention of the fiber-reinforced mortar and the water retention of the unreinforced mortar corresponds to the amount of water retained by the fibers.

3.2.1 Technical procedure

The test apparatus consists in two glass plates of 200 mm x 200 mm x 5 mm, one filter paper plate of 190 mm x 190 mm x 2 mm, a nonwoven tissue of 185 mm in diameter, a conical plastic ring of 140 mm smaller and 150 mm larger inside diameter and 12 mm in height. It is worth noting that the temperature and the relative humidity of both the

Preprints (www.preprints.org) | NOT PEER-REVIEWED | Posted: 20 July 2021 doi:10.20944/preprints202107.0431.v1

apparatus and the test room was verified to be about 20 °C and more than 50 %, respectively.

For the determination of the water retention, the water fraction W1 of the mixture has been set to 20%. First, one glass plate was weighted (m1). Second, the weight of the dry filter plate together with the glass plate was measured (m2). Thus, the nonwoven tissue was placed on top of the assembly dry filter plate-glass plate and they were weighted together (m3). Then, the plastic ring with its smaller opening downwards was put on top of the aforementioned assembly and the total weight was pointed out (m4). At this point, the mortar was placed in the plastic ring quickly and uniformly and the assembly was weighted (m5) and covered with a glass plate. Finally, the test arrangement was inverted and the filter plate was weighted (m6). The mass of the water absorbed by the filter is given by the difference between m7 = m6 – (m2 – m1). The mass of the absorbed water was measured at times t1= 3 min, t2= 10 min, t3= 60 min. Three procedures were carried on for: the unreinforced mortar (UR), the mortar reinforced with natural fibers Type 1 in the amount of 0.75% of the total weight (RM1) and the mortar reinforced with natural fibers Type 2 in the amount of 0.75% of the total weight (RM2).

Following figure 4 and figure 5 shown the typical test arrangement and the phases with which the amount of the absorbed water is determined.

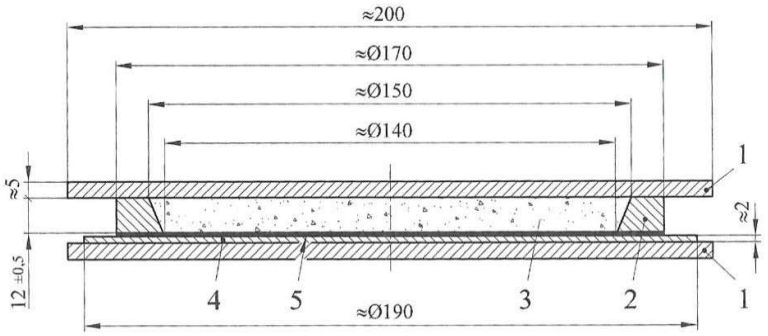

Figure 4. Typical test arrangement for determining the water retention of fresh mortar.

Figure 5. From the right: glass plate (GP), GP and filter paper plate (GFP), GFP and nonwoven tissue (GFPT), GFPT and plastic ring (GFPTR), GFPTR with fresh mortar placed.

3.3 Three-points bending test

Three points bending test (3PBT) was performed on several specimens of 160 mm in length, 40 mm in height and 40 mm in thickness. A notch with thickness t_n and depth a equal to 2 mm and 6 mm, respectively, was fabricated on the mortar sample, resulting with a notch to beam depth ratio a/d equal to 0.15 [23]. Figure 6 illustrates the scheme of the load and the boundary conditions related to the beam under 3PBT.

Preprints (www.preprints.org) | NOT PEER-REVIEWED | Posted: 20 July 2021 doi:10.20944/preprints202107.0431.v1

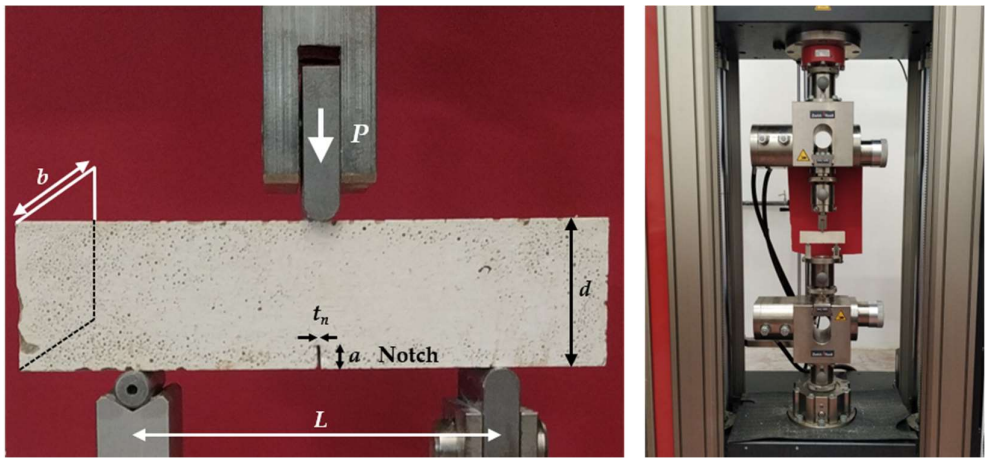

Figure 6. Pictures of the 3PBT carried out at the LPMS of L'Aquila. (**a**) Notched beam adopted in the tests; (**b**) setup of a specimen with the Zwick Roell hydraulic machine used for applying the load under displacement control.

The nominal distance between the supports was 100 mm, the width d and the thickness b were equal to 40 mm. The loading P, prescribed in displacement control conditions, was applied at the midspan of the beam. Two rollers at the bottom corresponded to the assigned boundary condition and allowed free horizontal movement.

The aim of the 3PBT is to determine the peak bending stress σf and the fracture energy Gf. Several approaches exist to determine the Gf, but the most widely valid formulation is the one recommended by RILEM, according to which the total energy G_f is given by the following expression:

$$G_f = \frac{W_0 + m \cdot g \cdot \delta_0}{(d-a)} \quad (1)$$

Where W_0 is the area subtended by the load-deflection curve, m is the weight of the beam between the two supports, calculated as the beam weight multiplied by 1/L, g is the gravity acceleration, δ_0 is the deformation at the failure condition of the beam, b is the beam width, a is the notch-depth.

Next, the bending stress σ_f was computing according to the following equations:

$$\sigma_f = \frac{3 \cdot P \cdot L}{2 \cdot b \cdot (d-a)^2} \quad (2)$$

It is worth noting that for $P = P_{max}$ the previous equation gives the bending strength.

As already mentioned, all the tests were performed in displacement control condition by an hydraulic testing machine (Zwick Roell) in the Laboratorio Prove Materiali e Strutture (LPMS) in L'Aquila University. The samples were subjected to a vertical displacement imposed by setting a constant velocity of 0.5 mm/min. During the test both the Force P and *d*eflection d history were automatically recorded by the testing machine.

3.4 Tensile test

In this section, the splitting tests (ST) are illustrated aiming to measure the tensile strength of the samples. The splitting test procedure, also called Brazilian tests, in an indirect way of measuring the tensile proprieties of materials. Better than other direct ways of measuring the tensile capacity of the specimens, splitting procedure has the advantage that can easily be performed on the specimens, the scattering of data are very low, the suitable shapes of the samples can have a large variety of configurations, as cylinders, prisms, cubes. ST provides the sample to be compressed with a load concentrated on a pair of antipodal points. In this way, tensile stresses are induced perpendicularly to the applied load, with a magnitude proportional to the applied load.

Preprints (www.preprints.org) | NOT PEER-REVIEWED | Posted: 20 July 2021 doi:10.20944/preprints202107.0431.v1

When the internal stresses exceed the tensile strength, a crack triggers at the geometric center of the sample, in accordance with Griffith criterion [59]. If the trigger of the fracture does not happen in the geometrical center of the specimen, the ST can not be accepted as representative of the tensile capacity of the sample. Moreover, ST provides the fracture to be vertical and should be included within the two compressed point where the external load is applied.

In this study, ST is performed on 40 mm x 40 mm x 80 mm prismatic mortar specimens obtained from the two-half specimens representing the broken pieces of the 3PBT, as shown in figure 7.

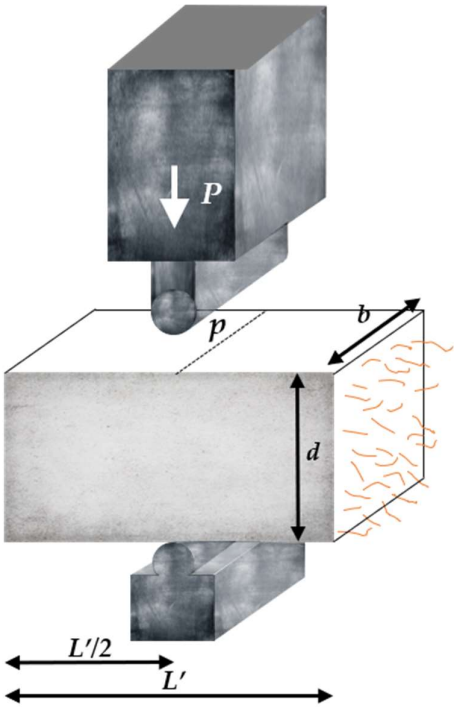

Figure 7. Setup of the tensile test carried out with the Zwick Roell machine under displacement control at the LPMS of L'Aquila.

The specimens were loaded at a constant displacement rate of 0.5 mm/min. All the test were carried on in the LPMS in the L'Aquila University. Both the force P and the vertical displacement δ were directly recorded by the test machine.

Then, the tensile stress f_t can be computed by using the following equation:

$$f_t = \frac{2 \cdot P}{\pi \cdot b \cdot d} \tag{3}$$

In the previous expression, when the load P reaches the maximum value P_{MAX}, the tensile strength can be computed.

3.5 Compression test

This section shows the compressive tests carried out on the fiber reinforced mortar specimens aiming to understand their compressive strength. The dimensions of the prisms were 40 mm x 40 mm x 80 mm, and this sample were one of the two-half specimens resulting from the 3PBT.

The detail of the test apparatus, the loading configuration and the assigned boundary conditions are illustrated in Figure 8.

Preprints (www.preprints.org) | NOT PEER-REVIEWED | Posted: 20 July 2021 doi:10.20944/preprints202107.0431.v1

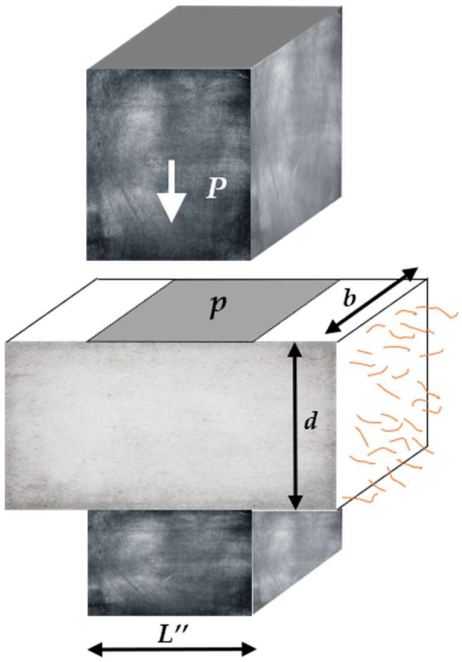

Figure 8. Setup of the compressive test carried out with the Zwick Roell machine under displacement control at the LPMS of L'Aquila.

The distributed load P was applied on a squared area of 40 mm x 40 mm, while the specimens were placed on a squared area of 40 mm x 40 mm on their bottom side. The compressive tests were performed in displacement control conditions with a constant displacement rate of 1 mm/min.

To compute the compressive stress, the following equation can be adopted:

$$f_c = \frac{P}{b \cdot L''} \tag{4}$$

When $P=P_{MAX}$ the compressive stress represents the compressive strength.

Moreover, using the following equation it is possible to compute the vertical strain ε_v:

$$\varepsilon_v = \frac{\delta}{d} \tag{5}$$

3.6 Tensile test of Sisal strands

This section shows the tensile tests carried out on the Sisal fibers strands, in order to define the tensile strength. Fifty cm length and 3 mm diameter of fibers samples were used to determine the tensile strength of the Sisal.

All the specimens have been tested for tensile strength and tensile elastic strains by means of Zwick Roell testing machine. All the results were recorded by dedicated software directly in Newton and millimeter units. The average specimens diameter was measured by means of micrometer and their gauge length were measured by means of a tape measure. The first tests have failed because the pressure required to avoid the wire sliding induced fiber tearing and thus the cut in correspondence to the machine clamps.

This means that the sliding failure happened before the maximum strength of the fiber has been reached. To overcome these drawbacks, the specimen was fixed between two pieces of wood with epoxy adhesive as shown in Figure 9. This adjustment allowed to carry out a representative number of tests reaching the tensile failure of the fibers and therefore characterizing its tensile strength.

Preprints (www.preprints.org) | NOT PEER-REVIEWED | Posted: 20 July 2021 doi:10.20944/preprints202107.0431.v1

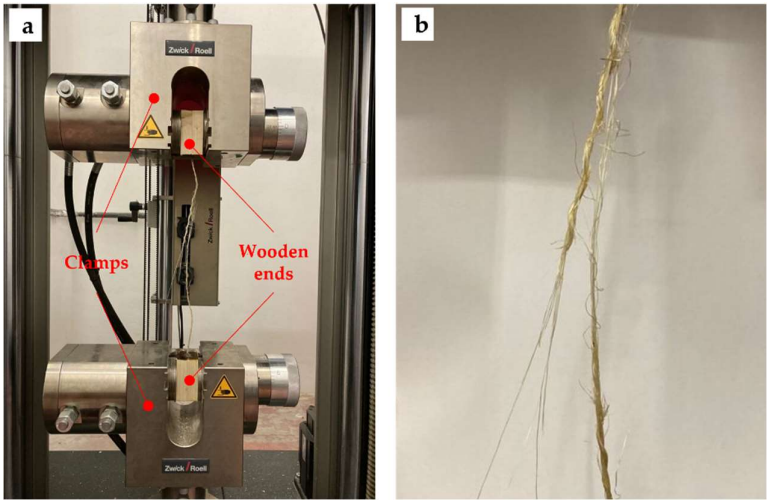

Figure 9. Setup of the tensile test of the strands carried out with the Zwick Roell machine under displacement control at the LPMS of L'Aquila. **a**) in evidence the wooden ends protecting the strands by tearing due to the pressure of the clamps; **b**) typical tensile failure of the strands.

4. Test results, discussion and further development

The results of the water retention tests are presented in following three tables and figure 10, regarding two types of fibers extracted from the woven fabric and reels, hereinafter briefly called RM1 and RM2, respectively. In particular, table 4 shows the results for the water retention test performed on the unreinforced mortar (UR), table 5 provides the results of the water retention test performed on the mortar reinforced with RM1 dispersed fibers and table 6 reports the results of the water retention test performed on the mortar reinforced with the RM1 dispersed fibers.

Table 4. Results of the water retention test performed on the unreinforced mortar.

	m_1 [g]	m_2 [g]	m_3 [g]	m_4 [g]	m_5 [g]	m_6 [g]	m_7 [g]	wr [%]
t_3	578.76	600.69	601.35	686.49	998.22	23.00	1.07	96.66
t_{10}	589.03	611.71	612.38	697.81	1030.67	24.59	1.91	95.35
t_{60}	581.25	603.62	604.34	689.99	1051.61	25.75	3.38	93.20

Table 5. Results of the water retention test performed on the mortar reinforced with RM1 dispersed fibers.

	m_1 [g]	m_2 [g]	m_3 [g]	m_4 [g]	m_5 [g]	m_6 [g]	m_7 [g]	wr [%]
t_3	578.72	601.14	601.77	686.91	1012.89	22.75	0.33	98.23
t_{10}	589.02	611.04	611.73	697.18	1024.90	22.61	0.59	97.66
t_{60}	590.26	612.35	613.01	698.66	1006.49	23.43	1.34	96.10

Table 6. Results of the water retention test performed on the mortar reinforced with RM2 dispersed fibers.

	m_1 [g]	m_2 [g]	m_3 [g]	m_4 [g]	m_5 [g]	m_6 [g]	m_7 [g]	wr [%]
t_3	581.07	603.78	604.48	689.58	1042.45	23.01	0.30	98.30
t_{10}	590.06	612.58	613.28	698.68	1059.00	23.15	0.63	97.79
t_{60}	578.58	600.48	601.16	686.77	1031.52	23.67	1.77	95.74

Preprints (www.preprints.org) | NOT PEER-REVIEWED | Posted: 20 July 2021 doi:10.20944/preprints202107.0431.v1

Figure 10 shows that the unreinforced mortar (UR) is characterized by a lower water retention than the mortar reinforced with both dispersed natural fibers, RM1 and RM2. In particular, the UR water retention is lower respect to RM1 and RM2 for all the considered times (t_1= 3 min, t_2= 10 min, t_3= 60 min). Moreover, the two reinforced mortar RM1 and RM2 show to retain a similar amount of water at times t1 and t2, whereas at time t_3 the mortar RM1 appears to retain more water than RM2. Focusing the attention to the fibers behaviors, the graph on the right of figure 10 shows that the RM2 fibers (named F_{RM2} in this graph) are characterized by a slightly greater water absorption than the RM1 fibers (named F_{RM1} in this graph) at the initial times t_1 and t_2, whereas at time t_3 F1 shows the highest water absorption (2.8 % vs 2.5 %).

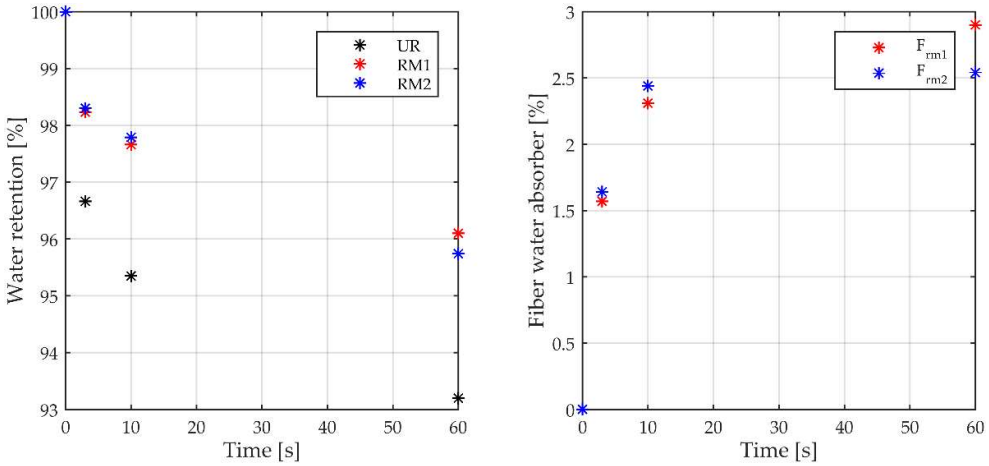

Figure10. On the left: results of the water retention test performed on the mortar reinforced with RM1 and RM2 dispersed fibers. On the right: the fiber water absorbed by the two fibers.

Figure 11 shows the results of the slump tests carried out for the mortar specimens strengthened by the F1 and the F2 fibers. Three percentages have been used in the analysis of fresh mortar, starting from 0.6%; for this reason, it was assumed a linear variation of the slump (indicated by the dotted lines) from the case of the unreinforced mortar (F= 0%) to the reinforced mortar with the lowest content fiber of 0.6%, as no tests were carried out in that range (0% – 0.6%).

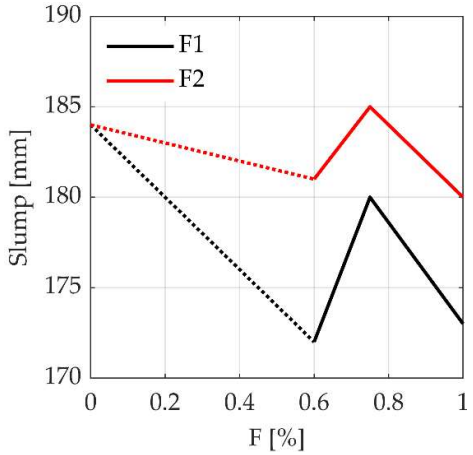

Figure 11. Slump test results for the fibers F1 and F2 by varying the fiber content *F*.

The curve trend in the figure 11 shows a first part between 0 and 0.6% where the workability of the fresh mortar gets worse for both fibers by increasing the fiber content,

 doi:10.20944/preprints202107.0431.v1

but is more evident for the fiber F1. For the F2 case, it is observed that no substantial difference in terms of slump by comparing the unreinforced case (0% of fibers) and the case with 0.6%.

In the range of 0.6 - 0.75% the slope of both curves inverts the sign and increases in a considerably matter, then come back to decrease for fiber content beyond 1.0%.

As a general remark, one can be note that the variation for all fiber content range 0-1.0% is characterized by a very small reduction of the slump for both types of fibers; in particular, we denote 3% for the type F1 and 7% for the type F2, against other type of fibers, for example the glass one for which the variation reaches 20%.

For the case of fresh mix strengthened by synthetic fibers, one can ben notes a constant decrease of the slump test values, relates to the compaction induced by the increasing of fibers percentage; in the present work where the natural fibers have been used, the greater water retention may have mitigated the compaction effect.

For the range 0.6-0.75% the increase for both fibers could be depending from the greater effect on the mix viscosity by the water absorption of the fibers respect to the compaction effect induced by the increase of the fiber content; beyond 0.75% the second one influences more than the first.

Moreover, the constant relative difference between the two fiber types may be due to their different aspect ratio. Indeed, the aspect ratio is inversely proportional to the number of fibers, so for the same fiber content F, a higher value of the aspect ratio leads to a lower number of fibers per unit volume of the fresh mix, as reported in the table 3. Hence, in the case of the natural fibers, the lower the number of fibers, the lower the workability of the product. Since the F1 fiber is characterized by the higher aspect ratio, as compared to the F2 fiber, one can observe a lower workability of the fibrous mortar.

This behavior can certainly be of interest, but to be extended as general rule must be further investigated.

However, it is also worth noting that the variation found for the slump values is certainly affected by scattering, that can be strongly reduced by a larger test campaign. Because of these remarks, we can assume that the workability of mortar mixed with natural fibers can be substantially independent from the fibers content.

The following figure 12 shows the relation between the Bending strength σ_f and the deflection of the prismatic specimen subjected to three-point bending tests (3PBT) with different fiber contents: it is recalled that 9 specimens are tested for each fiber content and both fibers F1 and F2. For the unreinforced case and the fiber content 0.75% with fibers type F1, 3 and 5 specimens are tested, respectively, for a total amount of specimens equal to 53.

In particular, the figure 12**a** illustrates the results of three tests on three unreinforced mortar specimens, with the mean value of the maximum Bending stress equal to 3.62 MPa. Moreover, the post peak behavior is characterized by a sharp brittle failure, as one would expect from unstrengthened mortar.

Conversely, the Figure 12**b-d** depicts the performances of the prismatic specimens in the reinforced configuration, by using two fibers (F1 and F2) and three different fiber content, according to the order 0.6%, 0.75% and 1.0%.

For a fiber content 0.6% one can see that the mortar strengthening by fibers, already with the lower content of fibers, gives important performance increasing for both Bending strength and ductility, especially for the fiber F1. It is worth noting the high level of the residual Bending stress after the peak, roughly equal to 50% and 30% of the peak for fiber type F1 and F2, respectively.

For a fiber content equal to 0.75% the two types of fiber show no strong differences in term of Bending stress, meanwhile the ductility is significantly different, decreasing for the fiber F1 and increasing for the fiber F2 respect the case 0.6%.

For the last case with the fiber content of 1.0%, one can see that the highest increasing of both Bending stress and ductility performances, especially for the fiber F1, that shows

Preprints (www.preprints.org) | NOT PEER-REVIEWED | Posted: 20 July 2021 doi:10.20944/preprints202107.0431.v1

a very small decrease of the residual bending stress after the peak, estimated equal to only 10% and then goes on up to the final displacement by small decreasing of stresses.

From the remarks of these results, it can be deduced that: i) the increasing in fiber content increases the peak of bending stress of shorter fiber F2 and the ductility of fiber F1; ii) highest values of fiber content reduce by a lot the brittle behavior of the mortar reinforced with fiber F1; iii) though the fiber F1 has less fibers per unit volume and one would expect less bending strength, it shows the highest value of the bending strength. This may be due to the greater superposition of the longer fibers that cover better all the length of the specimen, ensuring a greater number of fibers in the cracked section respect the smaller ones.

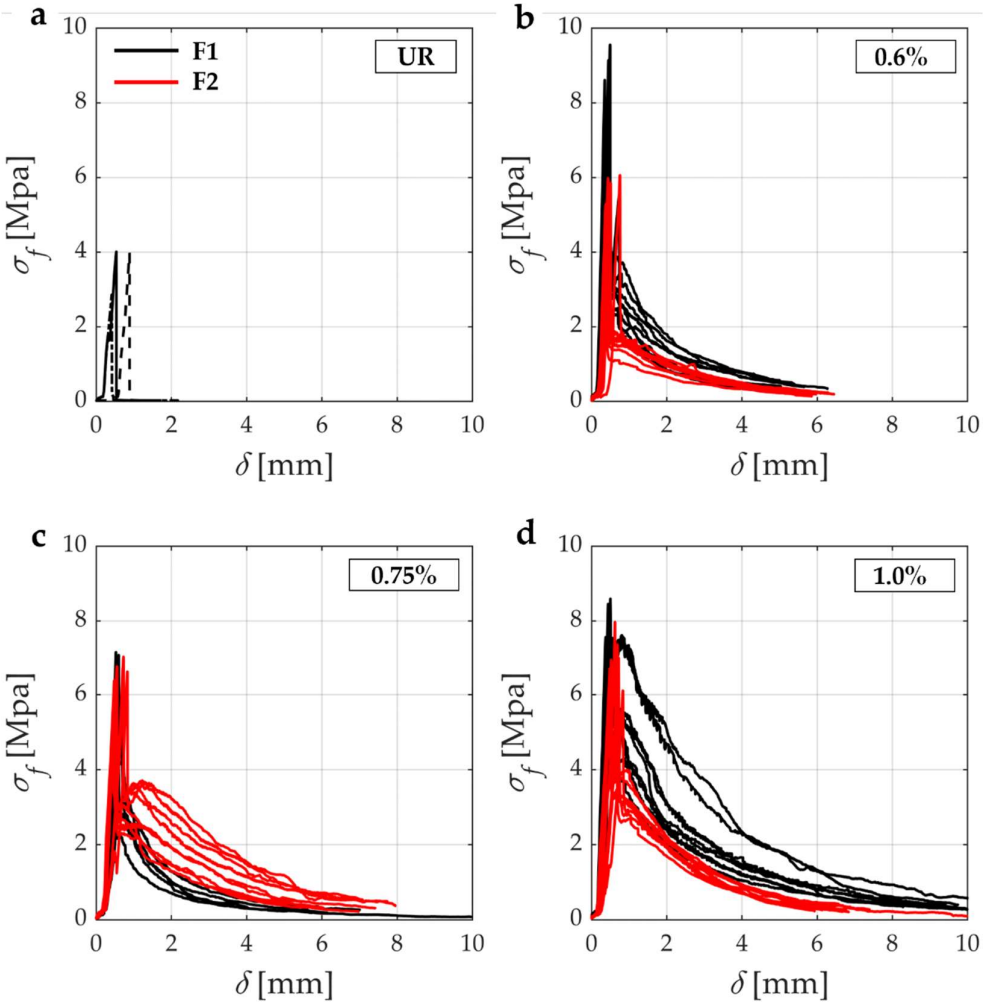

Figure 12. Bending strength σ_t related to the vertical displacement in the 3PBTs for: **a**) unreinforced case (UR). Reinforced cases by assuming two fiber types (F1 and F2) with fiber contents equal to: **b**) 0.6%; **c**) 0.75%; **d**) 1.0%.

Further information to better understand the influence of both fiber content and fiber type on the bending strength of the strengthened mortar are shown in the figure 13. In particular, the Figure 13**a** allows to evaluate the benefit of the reinforcement in term of bending performance σf with respect to the fiber content, by using the equation (2) for P= P_{max}.

Despite many uncertainties affect the scattering of the results (mixing time, failure mechanism, the order with which the components are added in mix), the improvement of bending strength is clear.

Preprints (www.preprints.org) | NOT PEER-REVIEWED | Posted: 20 July 2021 doi:10.20944/preprints202107.0431.v1

Moreover, figure 13**b** shows the trend of the fracture energy Gf, as the fiber content F varies. G_f is computed by using the equation (1), that takes into account the amount of energy dissipated to generate cracks per unit area, until to bending strength is reduced to almost zero. In this case the fracture energy shows no strong difference between the two fibers F1 and F2, while just for the fiber content greater than 0.75% starts to invert the trend.

In particular, starting from the fiber content equal to 0.8%, the F1 fiber begins to provide an ever-greater fracture energy, while the curve regarding to the F2 fiber shows the opposite trend; for fiber content equal to 1.0% the fracture energy computed for the F1 is equal to 1.85 times the one computed for the fiber F2. It is worth noting the following experimental evidences: i) the slope of the curve related to fiber F1 shows a slope significantly greater than the one of the fiber type F2; ii) the curves in the two graphs of the figure 12 have two intersections in the same fiber content range.

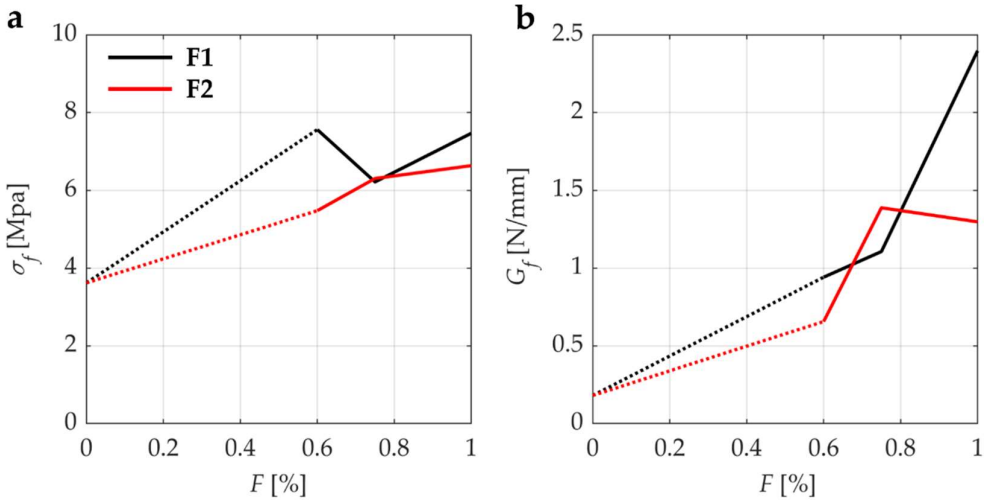

Figure 13. a) Bending strength σf and **b**) fracture energy Gf measured in the 3PBT for two fiber type F1 and F2 with different fiber content.

The following figure 14 shows the relation measured between the tensile stress σ_f and the deflection δ obtained for the unstrengthened and strengthened mortar specimens under the Brazilian Test (BT).

It is recalled that these tests were performed on one of the two half parts in which the specimens were broken from the previous 3PBTs; the final number of specimens is 53 (half specimens).

For the unreinforced case of figure 14**a**, the average value of the tensile strength is equal to 1.75 MPa. If compared with bending strength computed for the 3PBTs, this last is 2.07 times higher than the tensile strength.

As already denoted for the unreinforced specimens under the 3PBTs, the failure behavior is also in this case brittle, though it shows a greater displacement capacity. This phenomenon may be due to different engaging of the section, partialized in the 3PBT and fully reactive for tensile one.

Again in this case we can see the greater strength of the specimens with fiber F1, thus with the lower number of fibers per unit volume. This result matches the one obtained in the case of 3PBT and may confirm the hypothesis done.

Preprints (www.preprints.org) | NOT PEER-REVIEWED | Posted: 20 July 2021 doi:10.20944/preprints202107.0431.v1

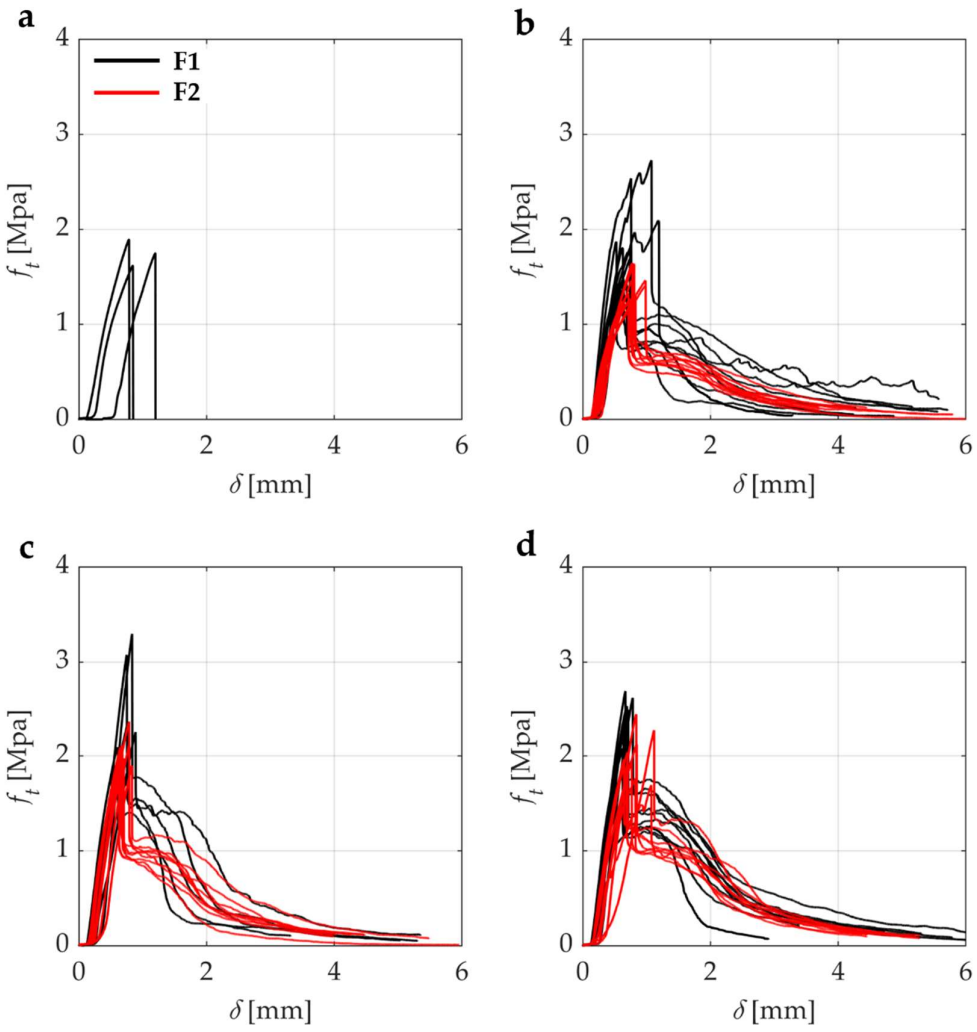

Figure 14. Tensile stress f_t related to the vertical displacement in the BTs for: **a**) unreinforced case (UR). Reinforced cases by assuming two fiber types (F1 and F2) with fiber contents equal to: **b**) 0.6%; **c**) 0.75%; **d**) 1.0%.

Further information for better understanding the influence of both fiber content and fiber type on the tensile strength of the strengthened mortar are shown in the figure 14. In particular, the Figure 14a allows to evaluate the benefit of the reinforcement in term of tensile strength f_t with respect to the fiber content, computed by using the equation (3) for P=P_{max}.

Preprints (www.preprints.org) | NOT PEER-REVIEWED | Posted: 20 July 2021 doi:10.20944/preprints202107.0431.v1

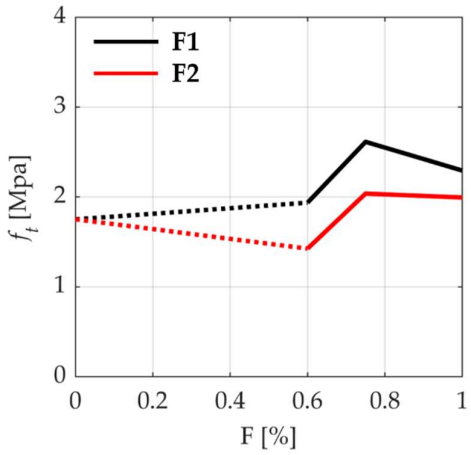

Figure 15. Tensile strength f_t measured in the BTs for two fiber type (F1 and F2) with different fiber content.

Compared with the 3PBT at the same fiber content, the bending strength is 3.25 times the tensile strength.

Regarding the fiber F2, one can observe a decrease in the tensile strength, although not marked, up to achieve 1.43 MPa for F= 0.60%; from here the tensile strength goes up suddenly to 2.04 MPa for F =0.75%, then it keeps almost constant up to achieve 2.00 MPa for F= 1.0%.

By comparing that value with the bending strength computed for the same fiber content (F= 1.0%) one can see the same difference found for the previous fiber content 0.75% (indeed σ_f is 3.3 times f_t).

Once again from figure 15 one can see the same trend of the figure 13**a**: the F1 fiber type leads to the higher performance respect to the fiber F2. It is worth nothing that this result is reached with the shorter fiber and lower aspect ratio, as compared to the F2 fiber. This result seems to be against the trend of mortar strengthened by synthetic fibers, for which the shorter fiber usually gives better tensile strength (also seems logical since the shorter fibers are almost twice respect the longer ones, reaching higher distribution of the fibers over the entire specimen and thus higher number of fibers where crack opens).

Since this trend is clear for both bending and tensile strength for all fiber contents, the phenomenon might be specific for the natural fibers and it may be attributed to the trend of fibers to agglomerate; this imply that the effective number of fibers drastically decreases, because just a part is in contact with the mortar on all surface and thus can exploit the maximum adhesion.

To support this hypothesis, we can observe the trend of fiber F1 in the figure 13**a** and 15: from the fiber content equal to 0.75% the longer ones begin to significantly decrease their performance for the decrease of the effective number of fibers (binder effect).

Greater quantity of fluidizer (now equal to 0.2%, see table 3), may improve the dispersion of the fibers decreasing the binder effect, but this may get worse the workability.

The following figure 16 shows the relation measured between the compressive stress f_c and the vertical strain ε_v obtained for the unstrengthened and strengthened mortar specimens under Compression Tests (CT).

Plots of figure 16**a** refer to 6 specimens. In this case the mean value of the compressive strength is equal to 12.76 MPa and one can also see a sudden drop of the strength after reaching the peak, typical of the quasi-brittle materials.

Figures 16**b-d** show the relationship between f_c and ε_v obtained for the strengthened mortar specimens tested under Compression Test (CT) for different fiber content percentage F.

Preprints (www.preprints.org) | NOT PEER-REVIEWED | Posted: 20 July 2021 doi:10.20944/preprints202107.0431.v1

The tests on strengthened configuration have been caried out on 9 specimens, except for the set concerning the Fiber F1 with fiber content equal to 0.75%, for which 5 specimens have been tested. For all the sets of tested specimens one can observe an enhancement of the compressive strength, even if limited as compared to the contribute offered by the fibers in the other mechanical properties. Furthermore, on the contrary of the same test conducted on mortar strengthened with synthetic fibers, one can observe a limited scattering, especially for the fiber F1 with fiber content 0.6% and 0.75%.

As already remarked for the results in the previous tests, the higher value of fiber content seems to lead to a lower efficiency due to the lower number of fibers engaged in the resistant mechanism.

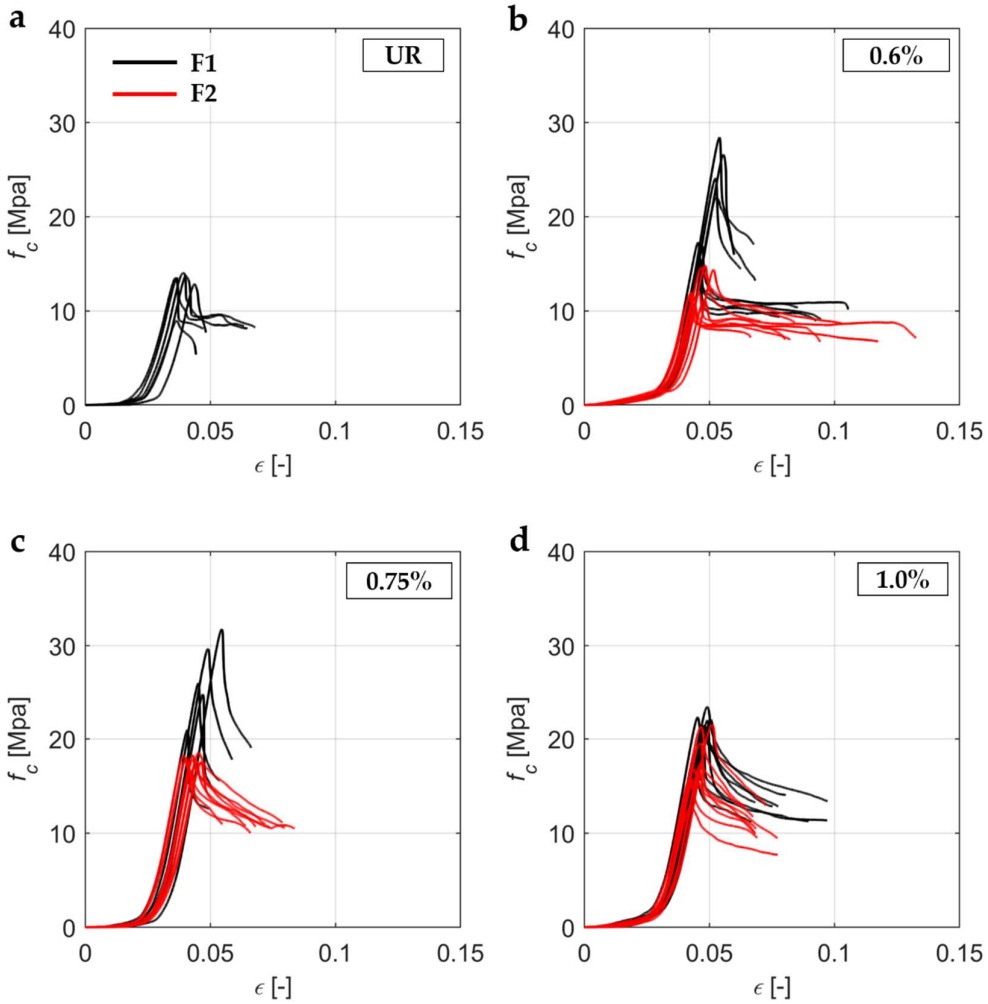

Figure 16. Compressive stress f_c related to the vertical strain ε_v measured in the CTs for: **a**) unreinforced case (UR). Reinforced cases by assuming two fiber types (F1 and F2) with fiber contents equal to: **b**) 0.6%; **c**) 0.75%; **d**) 1.0%.

Further information for better understanding the influence of both fiber content and fiber type on the compressive strength of the strengthened mortar are shown in the figure 16. In particular, this figure shows the variation of the compressive strength $f_{t'}$ computed by using the equation (4) for P=P_{max}, as function of the fiber content.

The results obtained in the CTs confirm definitely the trend given by the bending and tensile strength tests.

In particular, tensile and compressive tests have almost the same shape, to the point of being almost overlapping in all fiber content range.

Preprints (www.preprints.org) | NOT PEER-REVIEWED | Posted: 20 July 2021 doi:10.20944/preprints202107.0431.v1

In the case of compressive tests, the shape is a bit different, because the more the fiber content increases, the more the compressive strength increases, except for fiber content equal to 0.75% where the strength decreases for the fiber F1 and then it gets back to goes up.

An important phenomenon that it is worth to note is the better performance for the fiber F1. Indeed, bending, tensile and compressive strength are significantly higher in this case and only the slump test leads to better workability, but with quite difference, for the fiber F2. This means a substantial independence from the fiber content, suggesting the fiber type F1 with fiber content equal to 0.75% the best balance among the investigated combinations.

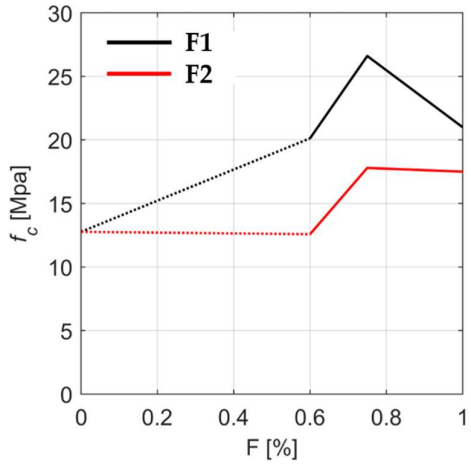

Figure 17. Compressive strength f_c measured in the CTs for two fiber type (F1 and F2) with different fiber content.

The following figure 18 summarizes the results obtained by the 3PBTs, the BTs and the CTs. In particular, this figure shows the increase, in percentage, in the bending strength σ_f, fracture energy G_f, tensile strength f_t and compressive strength f_c as compared to the unstrengthened case.

In term of absolute value, the best benefit as a result of the introducing fiber therein the mortar matrix, is observed in the fracture energy spent to open the crack in the specimens reinforced with fibers type F1 and fiber content equal to 1.0%.

This means that this type of fiber gives highest ductility, coupled with high bending strength, as depicted in figure 18**a-b.**

As already noted, the figure 18 shows that the fibers F1 have generally better performances in term of strength, especially for the fiber content equal to 0.75%, i.e. when the agglomerate of the fibers is limited, allowing to engage the maximum number of fibers.

On the contrary, the specimens reinforced with fiber F2 with lower fiber content, showed a worsening of the tensile and compressive strength, although not in substantial manner.

After analyzed all the results and compared the different combinations each other, neglecting the well note sources of uncertainties (irregularity of the cross-section, presence of micro-cracks, misalignment of the samples respect to their mid-thickness, different thickness of the specimens, spatial randomness of material properties), we can observe that the variability of the results in the case of the mortar reinforced by natural fibers may be due in particular to: i) the spatial orientation of the fiber which could help the longer fibers to intercept the crack position with higher probability; ii) the tendency of natural fibers to agglomerate more easily, reducing the number of effective fibers; iii) the higher water absorption that allows better workability but less mechanical strength.

Preprints (www.preprints.org) | NOT PEER-REVIEWED | Posted: 20 July 2021 doi:10.20944/preprints202107.0431.v1

As final remark, the use of fiber F1 is more recommendable as the coating in the retrofitting interventions, while the percentage of fiber content should be chosen according to the strength and/or ductility that one would want.

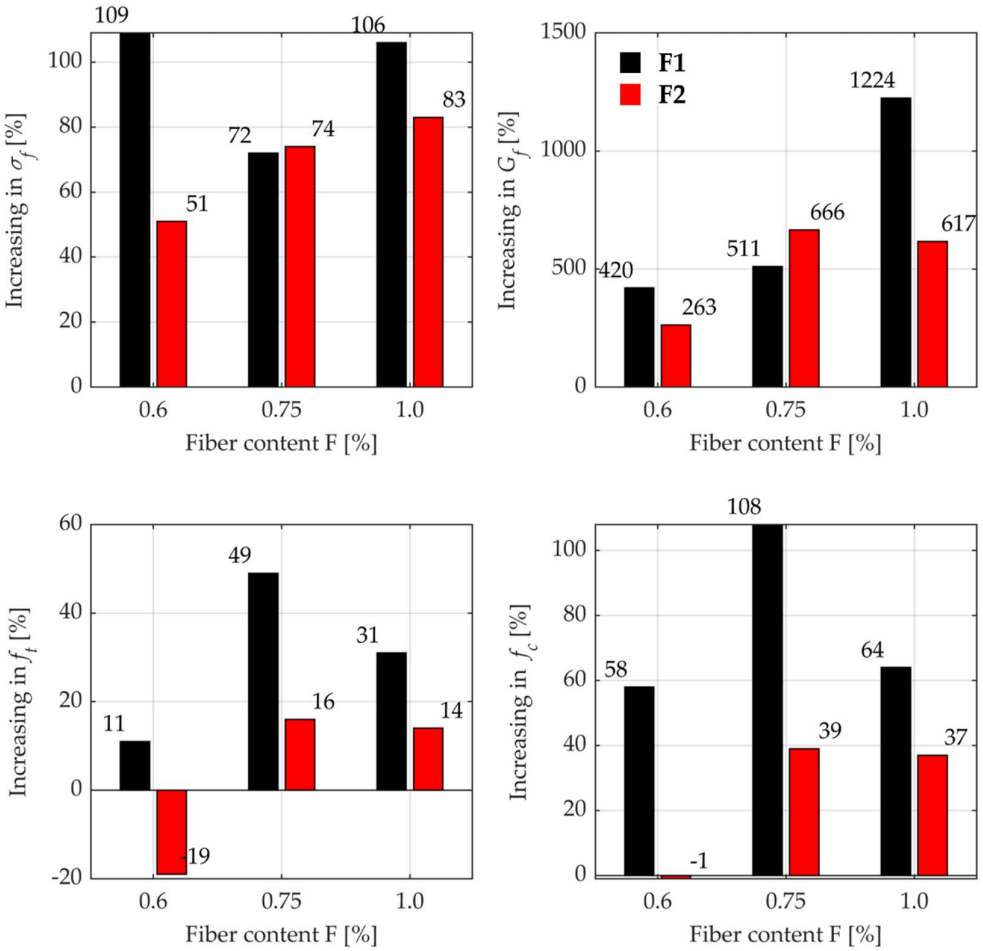

Figure 18. Increasing of the mechanical properties in the case of, **a**) bending strength $\sigma f.$; **b**) fracture energy G_f; **c**) tensile strength f_t and, **d**) compressive strength f_c, respect to the unreinforced case by varying the fiber content. The bars are coupled by type of fiber and are distinguished by color, black and red for the fibers F1 and F2, respectively, to simplify the comparison.

The following figure 19 shows the last tests carried out on the Sisal strand, with the aim to evaluate the ultimate strength of both strand and wire.

Tests were carried out under displacement control on two specimens, with displacement rate set on 0.1mm/sec, a speed enough to catch the failure of the single wire, with which evaluate, from theoretical point of view, the contribution of the fibers in the tests performed in the present work.

Preprints (www.preprints.org) | NOT PEER-REVIEWED | Posted: 20 July 2021 doi:10.20944/preprints202107.0431.v1

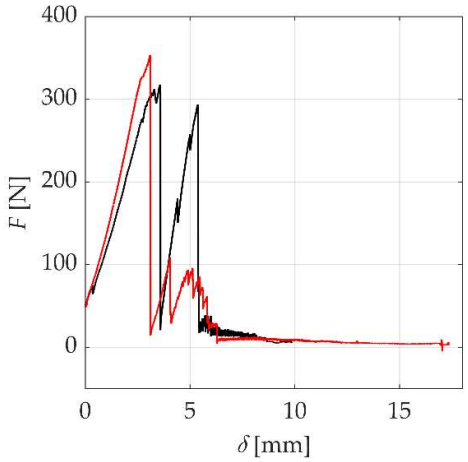

Figure 19. Tensile force *F* measured in the Sisal strand tensile tests for two specimens.

Two tensile tests on the Sisal strand provided results very close to the ultimate strength given by technical datasheet and literature.

After the peak force, one can see that the force decrease proceeds by small jumps and it is possible to check that they refer to the failure of single yarn, thanks also to direct view of the phenomenon. Hence, analyzing the data of the testing specimens for displacement greater than 6 mm, it was possible to evaluate the average failure tensile strength for a single wire equal to 8 N. With the nominal area of the single yarn equal to 0.06 mm^2 (taken from table 3), one can evaluate the ultimate tensile strength equal to 133 MPa, very close to both literature (130 MPa) and technical datasheet values (127 MPa). Obviously this value is affected by strong uncertainties (fibers diameter, for example), but the obtained results can be judged amazing if we think that they came from just two test.

For the purpose of an analytical evaluation of the contribution of the fibers, that can also help to better understand the effective number of the fibers that cross the crack, the following simplify procedure has shown.

As an example, we consider the case of the tensile test, whose results are summarized in the figure 15.

For the UR case the tensile strength is equal to 1.75 MPa, while for the strengthened mortar with fiber F1 and fiber content 0.75 the tensile strength is equal to 2.61 MPa.

This means that the contribution of the fibers is 0.86 MPa, the difference of the previous values. The total tensile force taken by the fibers can be evaluated as, $0.86 \cdot 40 \cdot 40 = 1376$N. Considering the experimental ultimate tensile strength of the fiber equal to 8N, the number of the effective fibers that cross the crack is 172.

Assuming the same number of fibers for any section where the crack opens (uniform distribution) and a small overlapping among the fibers (equal to 1.5 for both end), the expected value of the total number for the mortar mix with fiber F1 and fiber content equal to 0.75 is 2752, which is very close to the real one, as compared with the values of table 3.

The following figure 20 shows different specimens after the 3PBT, highlighting the fibers that cross the crack.

One can observe that the specimens with fibers type F2 (figure 20**a-b**) have a greater number of fibers, as compared to the ones with fiber type F1 (figure 20**c-d**).

Sometimes, by direct observation, it has been found also a greater fibers concentration in the center part of the specimens. Could be interesting to investigate possible correlations among the design parameters and this phenomenon.

Preprints (www.preprints.org) | NOT PEER-REVIEWED | Posted: 20 July 2021 doi:10.20944/preprints202107.0431.v1

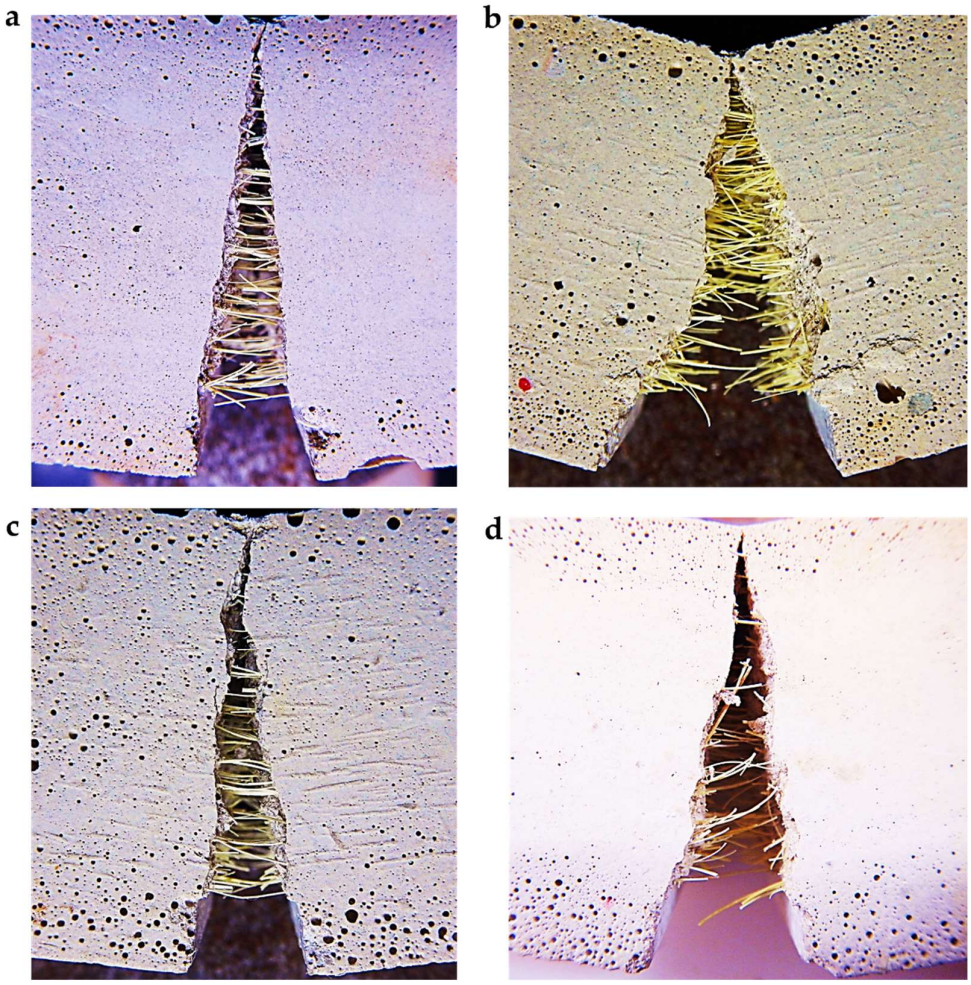

Figure 20. Cracks after the 3PBTs. **a**) Fibers F2-0.6%; **b**) Fibers F2-1.0%; **c**) Fibers F1-0.6%; **d**) Fibers F1-1.0%.

6. Conclusions

This work presents a study on the use of the natural fibers Sisal, extracted from Aloe plants, in the strengthening of masonry buildings and brick structures, especially when the intervention regards cultural heritage. Indeed, here the attention to the preservation of the ancient structures is very high and poses important limitations in term of strategies and materials that can be used.

The study aims to investigate the mechanical properties of the mortar reinforced with three different fiber content – 0.6%, 0.75%, 1.0% - and two type of fiber, named F1 and F2, with 13 mm and 24 mm length, respectively.

A total of 53 specimens have been tested at the LPMS of L'Aquila with the Zwick Roell machine; specimens are tested under displacement control and subjected to 3PBTs, BTs, CTs. Two Sisal strands have been pulled with the same machine under displacement control, with the aim to compare the experimental ultimate tensile strength of strand and yarn with both literature and technical data provided by manufacturer.

Regarding the workability, the slump test had highlighted a substantially independence from the fibers content of the mortar mixed with Sisal. Indeed, the variation between the lowest and the highest value of the slump test is 3% and 7% for fiber type F1 and F2, respectively.

As expected, the experimental results on the specimens at the end of aging, showed that the addition of short fiber in the mortar, provides a great increase of the mechanical properties, especially for what regards the ductility, measured by the fracture energy spent to open the crack. Indeed, one can see the highest increase among all performed tests, up to 1200% in the case of mortar with fiber F1 and fiber content equal to 1.0%, as compared with UR case.

The same type of fiber gives again the better performances for bending, tensile and compressive strength for almost all fiber content, especially for the 0.75%.

Conversely, the specimens characterized by fiber F2 with lower fiber content, did not show an improvement of both the tensile and the compressive behaviors, although the decreasing of both the tensile and the compressive strength was not substantial. This phenomenon can be due to the tendency of the Sisal fiber to agglomerate when the number of fibers becomes larger; the observed agglomeration can be the cause for the decreasing in the number of effective fibers and the overall lower strength.

The results also gave important information about the mechanical behavior of the specimens reinforced with Sisal, highlighting particular phenomena mainly attributable to the use of Sisal natural fibers.

After analyzed all the results and compared the different combinations each other, neglecting the well note sources of uncertainties (i.e. irregularity of the cross-section, presence of micro-cracks, misalignment of the samples respect to their mid-thickness, different thickness of the specimens, spatial randomness of material properties), we can observe that the variability of the results in the case of the mortar reinforced by natural fibers may be due in particular to: i) the spatial orientation of the fiber which could help the longer fibers to intercept the crack position with higher probability; ii) the tendency of natural fibers to agglomerate more easily, reducing the number of effective fibers. This affects especially the mix with higher fiber content; iii) the higher water absorption that allows better workability but lower mechanical strength.

For what concerns the tensile behavior, the performed tests have showed a significant increase for both the tensile strength and ductility and it is worth underlying that this result is remarkable, since this type of retrofitting for masonry structures mostly aims to carry tensile stresses.

Moreover, the tested material ensures the full compatibility from physical and chemical point of view with the original material of the ancient buildings.

As final remarks, the use of fiber F1 is more recommendable as the coating in the retrofitting interventions, especially for historical buildings, while the percentage of fiber content should be chosen according to the strength and/or ductility that one would want to reach.

Given the importance of the use of green technology to reduce the carbon foot print in the world of the building, the authors will focus their next researches on the geocomposites and other green technology that uses waste material to improve the earthquake performance of structures, as well as further investigate some phenomena emerged in this study and still not clear, as the tendency of natural fibers to agglomerate.

Author Contributions: Conceptualization, methodology, software, validation, formal analysis, investigation, data curation, writing-original draft preparation, visualization, M. Vailati; investigation, data curation, validation, M. Mercuri; writing-review and editing, M. Angiolilli, A. Gregori and M. Mercuri; validation, supervision, project administration, funding acquisition, A. Gregori;

Funding: this research was carried out thanks to the funding PON research and innovation 2014-2020.

Acknowledgments: The authors gratefully acknowledge the support of the "Aquilaprem S.r.l." company (L'Aquila, Italy) for the concession of materials as well as Dr. Paolo Dacci and Eng. Daniele Martini for the development of the mix-design of the product.

Conflicts of Interest: The authors declare no conflict of interest. The funders had no role in the design of the study; in the collection, analyses, or interpretation of data; in the writing of the manuscript; nor in the decision to publish the results.

References

1. Silva B, Dalla Benetta M, da Porto F, Modena C. Experimental assessment of in-plane behaviour of three-leaf stone masonry walls. *Construction and Building Materials* **2014**, 53, 149-61.
2. Vailati, M., Monti, G., Khazna, M.J., Realfonzo, R. and De Iuliis, M., 2016. Probabilistic seismic response analysis of existing masonry structures. *Proceedings of the 16th International Brick and Block Masonry Conference* **2016**, 2489–249
3. Calderini C, Cattari S, Lagomarsino S. In-plane strength of unreinforced masonry piers. *Earthquake engineering & structural dynamics* **2009**, 38(2), 243-67.
4. Menegotto M, Monti G, Salvini S, Vailati M. Improvement of Transverse Connection of Masonry Walls through AFRP Bars. *Advances in FRP Composites in Civil Engineering* **2011**, 947-950.
5. Ricci P, Di Domenico M, Verderame GM. Experimental assessment of the in-plane/out-of-plane interaction in unreinforced masonry infill walls. *Engineering Structures* **2018**, 173, 960-78.
6. Mercuri M, Pathirage M, Gregori A, Cusatis G. Computational modeling of the out-of-plane behavior of unreinforced irregular masonry. *Engineering Structures* **2020**, 223, 111181.
7. Khan, N.A., Monti, G., Nuti, C., Vailati, M. Effects of infills in the seismic performances of an RC factory building in Pakistan. *Buildings* **2021**, 11, 276. https://doi.org/10.3390/buildings11070276.
8. Mercuri M, Pathirage M, Gregori A, Cusatis G. On the collapse of the Medici masonry tower: an integrated discrete-analytical approach. *SPREE internal report* **2021**, No. 21-6/001S
9. Zhan, Y., Meschke, G. Multilevel computational model for failure analysis of steel-fiber–reinforced concrete structures. *Journal of Engineering Mechanics* **2016**, 142(11), 04016090.
10. Krevaikas, T. D., Triantafillou, T. C. Masonry confinement with fiber-reinforced polymers. *Journal of Composites for Construction* **2005**, 9(2), 128-135.
11. Corradi, M., Borri, A., Castori, G., Sisti, R. Shear strengthening of wall panels through jacketing with cement mortar reinforced by GFRP grids. *Composites Part B: Engineering* **2014**, 64, 33-42.
12. Angiolilli, M., Gregori, A., Pathirage, M., Cusatis, G. Fiber Reinforced Cementitious Matrix (FRCM) for strengthening historical stone masonry structures: Experiments and computations. *Engineering Structures* **2020**, 224, 111102.
13. Kouris, L. A. S., Triantafillou, T. C. State-of-the-art on strengthening of masonry structures with textile reinforced mortar (TRM). *Construction and Building Materials* **2018**, 188, 1221-1233.
14. Borri, A., Corradi, M., De Maria, A. The Failure of Masonry Walls by Disaggregation and the Masonry Quality Index. *Heritage* **2020**, 3(4), 1162-1198.
15. Angiolilli, M., Gregori, A. Triplet test on rubble stone masonry: numerical assessment of the shear mechanical parameters. *Buildings* **2020**, 10(3), 49.
16. Sisti, R., Di Ludovico, M., Borri, A., Prota, A. Damage assessment and the effectiveness of prevention: the response of ordinary unreinforced masonry buildings in Norcia during the Central Italy 2016–2017 seismic sequence. *Bulletin of Earthquake Engineering* **2019**, 17(10), 5609-5629.
17. Borri, A., Corradi, M., Castori, G., Sisti, R., De Maria, A. Analysis of the collapse mechanisms of medieval churches struck by the 2016 Umbrian earthquake. *International Journal of Architectural Heritage* **2019**, 13(2), 215-228.
18. Bakis, C. E., Bank, L. C., Brown, V., Cosenza, E., Davalos, J. F., Lesko, J. J., Machida, A., Rizkalla, S. H., Triantafillou, T. C. Fiber-reinforced polymer composites for construction—State-of-the-art review. *Journal of composites for construction* **2002**, 6(2), 73-87.
19. Papanicolaou, C. G., Triantafillou, T. C., Karlos, K., Papathanasiou, M. Textile-reinforced mortar (TRM) versus FRP as strengthening material of URM walls: in-plane cyclic loading. *Materials and structures* **2007**, 40(10), 1081-1097.
20. Valluzzi, M. R. Strengthening of masonry structures with fibre reinforced plastics: from modern conception to historical building preservation. *Structural analysis of historic construction* **2008**, 1, 33-45.
21. Lanas, J., Alvarez-Galindo, J. I. Masonry repair lime-based mortars: factors affecting the mechanical behavior. *Cement and concrete research* **2003**, 33(11), 1867-1876.
22. Alecci, V., De Stefano, M., Focacci, F., Luciano, R., Rovero, L., Stipo, G. Strengthening masonry arches with lime-based mortar composite. *Buildings* **2017**, 7(2), 49.
23. Angiolilli, M., Gregori, A., Vailati, M. Lime-based mortar reinforced by randomly oriented short fibers for the retrofitting of the historical masonry structure. *Materials* **2020**, 13(16), 3462.
24. Bentur, A., Mindess, S. *Fibre reinforced cementitious composites* **2006**, Crc Press.
25. Henshaw, J. M., Han, W., Owens, A. D. An overview of recycling issues for composite materials. *Journal of Thermoplastic Composite Materials* **1996**, 9(1), 4-20.

26. Conroy, A., Halliwell, S., Reynolds, T. Composite recycling in the construction industry. *Composites Part A: Applied Science and Manufacturing* **2006**, 37(8), 1216-1222.
27. Santos, S. F. D., Tonoli, G. H. D., Mejia, J. E. B., Fiorelli, J., Savastano Jr, H. Non-conventional cement-based composites reinforced with vegetable fibers: A review of strategies to improve durability. *Materiales de Construcción* **2015**, 65(317), 041.
28. Ramamoorthy, S. K., Skrifvars, M., Persson, A. A review of natural fibers used in biocomposites: plant, animal and regenerated cellulose fibers. *Polymer reviews* **2015**, 55(1), 107-162.
29. de Carvalho Bello, C. B., Boem, I., Cecchi, A., Gattesco, N., Oliveira, D. V. Experimental tests for the characterization of sisal fiber reinforced cementitious matrix for strengthening masonry structures. *Construction and Building Materials* **2019**, 219, 44-55.
30. Fidelis, M. E. A., De Andrade Silva, F., Toledo Filho, R. D. The influence of fiber treatment on the mechanical behavior of jute textile reinforced concrete. *In Key Engineering Materials* **2014** (Vol. 600, pp. 469-474).
31. Wambua, P., Ivens, J., Verpoest, I. Natural fibres: can they replace glass in fibre reinforced plastics?. *Composites science and technology* **2003**, 63(9), 1259-1264.
32. Cristaldi, G., Latteri, A., Recca, G., Cicala, G. Composites based on natural fibre fabrics. *Woven fabric engineering* **2010**, 17, 317-342.
33. Ticoalu, A., Aravinthan, T., Cardona, F. A review of current development in natural fiber composites for structural and infrastructure applications. *In Proc. of the southern region engineering conference (SREC 2010)* **2010**, pp. 113-117, Engineers Australia.
34. Begum, K., Islam, M. A. Natural fiber as a substitute to synthetic fiber in polymer composites: a review. *Research Journal of Engineering Sciences* **2013**, 2(3), 46-53.
35. Tolêdo Filho, R. D., Scrivener, K., England, G. L., Ghavami, K. Durability of alkali-sensitive sisal and coconut fibres in cement mortar composites. *Cement and concrete composites* **2000**, 22(2), 127-143.
36. Roma Jr, L. C., Martello, L. S., Savastano Jr, H. Evaluation of mechanical, physical and thermal performance of cement-based tiles reinforced with vegetable fibers. *Construction and Building Materials* **2008**, 22(4), 668-674.
37. Mukherjee, P. S., Satyanarayana K. G. Structure and properties of some vegetable fibres. *Journal of Material Science* **1984**, 19(12), 3925-3934.
38. Chand, N., Satyanarayana, K. G., Rohatgi, P. K. Mechanical characteristics of sunhemp fibres. *Indian Journal of Textile research* **1986**, Vol. 1, pp.86-89.
39. Razak, H. A., Ferdiansyah, T. Toughness characteristics of Arenga pinnata fibre concrete. *J. of Natural Fibers* **2005**, 2(2), 89-103.
40. Savastano Jr, H., Agopyan, V., Nolasco, A. M., Pimentel, L. Plant fibre reinforced cement components for roofing. *Construction and building materials* **1999**, 13(8), 433-438.
41. Al-Oraimi, S. K., Seibi, A. C. Mechanical characterisation and impact behaviour of concrete reinforced with natural fibres. *Composite Structures* **1995**, 32(1-4), 165-171.
42. Ramakrishna, G., Sundararajan, T. Impact strength of a few natural fibre reinforced cement mortar slabs: a comparative study. *Cement and concrete composites* **2005**, 27(5), 547-553.
43. Onuaguluchi, O., Banthia, N. Plant-based natural fibre reinforced cement composites: A review. *Cement and Concrete Composites* **2016**, 68, 96-108.
44. Li, Y., Mai, Y. W., Ye, L. Sisal fibre and its composites: a review of recent developments. *Composites science and technology* **2000**, 60(11), 2037-2055.
45. Bisanda, E. T. N., Ansell, M. P. Properties of sisal-CNSL composites. *Journal of Materials Science* **1992**, 27(6), 1690-1700.
46. Chand, N., Hashmi, S. A. R. Mechanical properties of sisal fibre at elevated temperatures. *Journal of Materials Science* **1993**, 28(24), 6724-6728.
47. Soroushian, P., Shah, Z., Won, J. P. Aging effects on the structure and properties of recycled wastepaper fiber cement composites. *Materials and structures* **1996**, 29(5), 312-317.
48. Olivito, R. S., Cevallos, O. A., Carrozzini, A. Development of durable cementitious composites using sisal and flax fabrics for reinforcement of masonry structures. *Materials and Design* **2014**, 57, 258-268.
49. De Andrade Silva, F., Toledo Filho, R. D., de Almeida Melo Filho, J., Fairbairn, E. D. M. R. Physical and mechanical properties of durable sisal fiber–cement composites. *Construction and building materials* **2010**, 24(5), 777-785.
50. Fujiyama, R., Darwish, F., Pereira, M. V. Mechanical characterization of sisal reinforced cement mortar. *Theoretical and Applied Mechanics Letters* **2014**, 4(6), 061002.
51. Lima, P. R., Toledo Filho, R. D., Melo Filho, J. A. Compressive stress-strain behaviour of cement mortar-composites reinforced with short sisal fibre. *Materials Research* **2014**, 17(1), 38-46.
52. De Carvalho Bello, C. B., Boem, I., Cecchi, A., Gattesco, N., Oliveira, D. V. Experimental tests for the characterization of sisal fiber reinforced cementitious matrix for strengthening masonry structures. *Construction and Building Materials* **2019**, 219, 44-55.
53. De Andrade Silva, F., Mobasher, B., Toledo Filho, R. D. Cracking mechanisms in durable sisal fiber reinforced cement composites. *Cement and Concrete Composites* **2009**, 31(10), 721-730.
54. Prasad, A. R., Rao, K. M. Mechanical properties of natural fibre reinforced polyester composites: Jowar, sisal and bamboo. *Materials and Design* **2011**, 32(8-9), 4658-4663.

 doi:10.20944/preprints202107.0431.v1

55. EN 1015-11: 2019. *Methods of test for mortar for masonry* - Part. 11: Determination of flexural and compressive strength of hardened mortar.
56. EN 1015-3:1999. *Methods of test for mortar for masonry* – Part 3: Determination of consistence of fresh mortar.
57. ASTM C1437-20. *Standard Test Method for Flow of Hydraulic Cement Mortar.*
58. UNI-EN 459-2:2010. *Building lime* – Part.2: Test methods.
59. . The phenomena of rupture and flow in solids (Philosophical transactions/Royal Society of London ser. A, v. 221) **1920**.